

MOLPHARM/2005/014035

Novel Potent *hERG* Potassium Channel Enhancers And Their *In Vitro* Antiarrhythmic Activity

Jun Zhou, Corinne E. Augelli-Szafran, Jenifer A. Bradley, Xian Chen, Bryan J. Koci, Walter A.
Volberg, Zhuoqian Sun, and Jason S. Cordes

Department of Safety Pharmacology, Pfizer Global Research and Development, Groton Laboratories,
Groton, CT 06340 (J.Z., J.A.B, X.C., B.J.K, W.A.V, Z.S, J.S.C); and CNS Chemistry, Pfizer Global
Research and Development, Michigan Laboratories, 2800 Plymouth Rd, Ann Arbor, MI
48105(C.E.A.S)

MOLPHARM/2005/014035

Running title:

Potent hERG enhancers: PD-118057 & analogues

Corresponding author:

Jun Zhou, MD, Ph.D.
Pfizer Global R & D
Groton Laboratories
M. S. 8274-1420
Eastern Point Road
Groton, CT 06340
Tel: 860-715 2413
Fax: 860-715 8093
E-mail: jun.zhou@pfizer.com

Stats:

Number of text pages:	29
Number of tables:	1
Number of figures:	8
Number of references:	23
Number of words in the Abstract:	250
Number of words in the introduction:	331
Number of words in the discussion:	889

Abbreviations: *hERG*: human *ether-à-go-go*-related gene; I_{Kr} : rapidly activating delayed rectifier potassium current; TdP: *torsades de pointes*; AP: action potential; APD: action potential duration; ECG: electrocardiogram; EAD: early afterdepolarization; LQTS: long-QT syndrome; CHF: congestive heart failure; TDR: transmural dispersion of repolarization

Abstract

A variety of drugs have been reported to cause acquired long-QT syndrome (LQTS) through inhibition of the I_{Kr} channel. Screening compounds in early discovery and development stages against their ability to inhibit I_{Kr} or the *hERG* channel has therefore become an indispensable procedure in the pharmaceutical industry. In contrast to numerous *hERG* channel blockers discovered during screening, so far only RPR260243 has been reported to enhance the *hERG* current. In this article, we describe several potent, mechanistically distinct *hERG* channel enhancers. One example is PD-118057 which produced average increases of 5.5 ± 1.1 , 44.8 ± 3.1 , and $111.1 \pm 21.7\%$ in the peak tail *hERG* current at 1, 3 and 10 μM , respectively, in HEK-293 cells. PD-118057 did not affect the voltage dependence and kinetics of gating parameters, nor did it require open conformation of the channel. In isolated guinea-pig cardiomyocytes, PD-118057 showed no major effect on I_{Na} , $I_{Ca,L}$, I_{K1} and I_{Ks} . PD-118057 shortened the action potential duration and QT interval in arterially perfused rabbit ventricular wedge preparation in a concentration-dependent manner. Presence of 3- μM PD-118057 prevented APD and QT prolongation caused by dofetilide. Early after depolarizations induced by dofetilide were also completely eliminated by 3 μM PD-118057. While further investigation is warranted to evaluate the therapeutic value and safety profile of these compounds, our data support the notion that *hERG* activation by pharmaceuticals may offer a new approach in the treatment of delayed repolarization conditions which may occur in inherited or acquired LQTS, congestive heart failure and diabetes patients.

Introduction

Drug-induced (“acquired”) long-QT syndrome, an effect manifested as prolongation of the QT interval on the surface electrocardiograph (ECG), has increasingly drawn attention from regulatory agencies and the pharmaceutical industry in recent years (De Ponti et al., 2000; De Ponti et al., 2001; Fermini and Fossa, 2003). The presence of delayed repolarization favors the genesis of early afterdepolarization (EAD) which can initiate an arrhythmia referred to as triggered activity (Zabel et al., 1997). Additionally, prolongation of the QT interval by drugs is often associated with an increased heterogeneity of cardiac repolarization (Antzelevitch, 2004), a potential substrate for a reentry mechanism responsible for the maintenance of arrhythmia. One particular type of arrhythmia, *torsade de pointes* (TdP), may cause syncope events and/or degenerate into ventricular fibrillation and death.

Since the majority of these drugs prolong the QT interval through inhibition of the rapidly activating delayed rectifier potassium current I_{Kr} , evaluating the propensity of a compound to inhibit this channel or its molecular counterpart, human *ether-à-go-go*-related gene (*hERG*) encoded channel, has become an indispensable screening procedure in drug development (Fermini and Fossa, 2003). Interestingly, the *hERG* channel appears to be the most promiscuous among all known voltage-gated potassium channels, with drugs from a wide range of chemical structures and therapeutic categories capable of inhibiting the channel (De Ponti et al., 2000; De Ponti et al., 2001). In the pharmaceutical industry, thousands of compounds are screened each day in the *hERG* assay, and an estimated 30% of compounds tested possess *hERG*-blocking activity to varying degrees. However, only one compound, RPR260243, has recently been reported (Kang et al., 2005) to enhance the *hERG* channel. This compound increases the *hERG* current mainly by slowing its deactivation kinetics. In this article, we report several new *hERG* channel enhancers with dramatic current-

MOLPHARM/2005/014035

enhancing effects and a distinct mechanism. PD-118057, as a representative among these compounds, is able to prevent and reverse QT-prolongation and associated arrhythmias (EAD) induced by a selective I_{Kr} blocker, dofetilide, in the arterially perfused rabbit ventricular wedge preparation.

Materials and Methods

All animal experiments were conducted in accordance with the regulations of the US National Institutes of Health (NIH Publication No. 8523, revised 1996) and European guidelines, and were approved by the Pfizer Institutional Animal Care and Use Committee.

Isolation of myocytes from guinea-pig hearts Ventricular myocytes were isolated from male Hartley guinea pigs using an enzyme-digestion method described previously (Cordes et al., 2005). In brief, a Langendorff heart was established and first perfused with oxygenated Ca^{2+} -free Isolation Solution (37°C) for 5 min. This was followed by perfusion with an enzyme-containing solution (collagenase type 2, Worthington; and protease, type XII, Sigma) for 8-10 minutes. The ventricles were then chopped into pieces in Storage Solution, filtered through a mesh and the cell suspension were stored at room temperature for at least one hour prior to use.

Patch-clamp recording Stable human embryonic kidney (HEK-293) cells expressing the *hERG* channel (Zhou et al., 1998) were licensed from Wisconsin Alumni Research Foundation or generated in house. Methods for cell culture and whole-cell patch-clamp studies on the *hERG* channel were reported previously (Cordes et al., 2005; Sun et al., 2004; Volberg et al., 2002). EPC-9 (HEKA Electroniks, Germany) or MultiClamp 700A (Axon Instruments, CA) amplifiers were employed to record the current, controlled by Pulse+PulseFit 8.40 (HEKA Electroniks, Germany) or pClamp 8.2 (Axon Instruments, CA) software through an interface. The *hERG*, I_{K1} and I_{Ks} currents were measured at 35°C (maintained by a TC-344B Temperature Controller, Warner Instruments, CT). I_{Na} , I_{Ca} and action potentials were recorded at room temperature. Voltage protocols used for eliciting each current are described in the text. Action potentials recorded from isolated myocytes were

MOLPHARM/2005/014035

elicited using the whole-cell configuration or perforated-patch technique when amphotericin B (120 ug/ml) was included in the pipette solution.

Wedge preparation study Under anesthesia by 30-35 mg/kg ketamine HCl (i.v.) following 5-mg/kg xylazine (i.m.), the heart from a female New Zealand White rabbit (2.5-5.5 kg) was removed and placed in cold (4-10°C) 95% O₂-5% CO₂ saturated cardioplegic solution (in mM): 129 NaCl, 24 KCl, 0.9 NaH₂PO₄, 20 NaHCO₃, 1.8 CaCl₂, 0.5 MgSO₄, and 5.5 glucose. The left main coronary artery or its major branch (normally circumflex branch) was cannulated and perfused with the cardioplegic solution to wash out the intravascular blood. A transmural left ventricular wedge from the anterior wall was dissected and the major leaking vessels ligated. The tissue was then placed in a tissue bath and perfused with 36 ± 0.5°C Tyrode's solution (mM): 129 NaCl, 4 KCl, 0.9 NaH₂PO₄, 20 NaHCO₃, 1.8 CaCl₂, 0.5 MgSO₄, and 5.5 glucose, pH 7.35 when buffered with 95% O₂ and 5% CO₂. The perfusion pressure was maintained at ~40 mmHg and monitored through a pressure transducer connected with the PowerLab/8SP Data Acquisition System (ADInstruments, Australia). The tissue was paced with ~150% suprathreshold stimuli at 1 Hz by a DS8000 Digital Stimulator (World Precision Instruments, FL) through platinum bipolar electrodes on the endocardial surface. Floating glass electrodes, with a resistance of approximately 10~20 MΩ when filled with 2.7 M KCl, were placed in the epicardial or endocardial myocardium, respectively. Action potentials from both sites were amplified through an IX2-700 Dual Intracellular Preamp (Dagan Corporation, MN). The transmural electrocardiogram (ECG) was recorded by using two Ag/AgCl electrodes placed ~1 cm away from epicardial and endocardial surfaces and fed into an EX1 Differential Amplifier (Dagan Corporation, MN). All the signals were monitored and recorded using Chart 5 software (ADInstruments, Australia) through the PowerLab/8SP system. An equilibrium period of at least 1-

MOLPHARM/2005/014035

hour was allowed in each experiment before any data collection. Action potential duration (APD) parameters were analyzed using Peak Parameter extension within the Chart 5 program.

Chemicals and Solutions For isolation of the myocytes, the calcium-free Isolation Solution was composed of (in mM): NaCl, 137; KCl, 5.4; HEPES, 10; MgCl₂·6H₂O, 1; NH₂PO₄·H₂O, 0.33; *d*-glucose, 10; pH 7.4 with NaOH. The Storage Solution contained (in mM): Glutamic acid, 50; EGTA, 0.5; Glucose, 10; HEPES, 10; KCl, 40; KH₂PO₄, 20; KOH, 70; MgCl₂·6H₂O, 3; Taurine, 20; pH to 7.4 with NaOH. For the *hERG* current recording from the *hERG*-HEK cells, the bath (Tyrode's) solution was composed of (in mM): NaCl, 137; KCl, 4; CaCl₂, 1.8; MgCl₂, 1; Glucose, 10; HEPES, 10; pH to 7.4 with NaOH. The pipette solution contained (in mM): KCl, 130; MgATP, 5; MgCl₂, 1; HEPES, 10; EGTA, 5; pH to 7.2 with KOH. For the recording of the calcium currents, the bath solution was composed of (in mM): Tris, 137; CaCl₂, 1.8; MgCl₂·6H₂O, 1; Glucose, 5; CsCl, 20; pH to 7.4 with CsOH. The internal pipette solution was composed of (in mM): CsCl, 125; MgATP, 5; HEPES, 10; EGTA, 15; TEA-Cl, 20; pH 7.2 with CsOH. For I_{K1} and I_{Ks} recording, bath solution contained (in mM): NaCl 137, KCl 5.4, CaCl₂ 1.8, MgCl₂ 1, HEPES 10, NaH₂PO₄ 0.33, glucose 10 (pH 7.4 with NaOH). CdCl₂ (250 μM) and dofetilide (1 μM) were added to block I_{Ca,L} and I_{Kr}, respectively. The pipette solution contained (in mM): K-aspartate 125, KCl 20, MgCl₂ 1, HEPES 5, EGTA 10, Mg-ATP 5 (pH 7.2 with KOH). For I_{Na} recording, the bath solution contained (in mM): NaCl 15, CaCl₂ 0.5, CsCl 4, MgCl₂ 1, TEA-Cl 125, CdCl₂ 0.25, HEPES 10, and glucose 10 (pH 7.4 with CsOH). Pipette solution was composed of (in mM): NaCl 5, CsOH 125, Aspartic acid 125, TEA-Cl 20, EGTA 10, HEPES 10, Mg-ATP 5 (pH 7.2 with CsOH). The bath solution used to record the action potentials was the Tyrode's solution, and the pipette solution contained (in mM): KCl, 130; MgATP, 5; MgCl₂, 1; HEPES, 10; EGTA, 5; Amphotericin B; 120 μg/ml; pH 7.2 with KOH.

MOLPHARM/2005/014035

All test compounds used in this study were synthesized at Pfizer Global Research and Development. Other chemicals were purchased from Sigma-Aldrich (St. Louis, MO). Compounds were dissolved in dimethyl sulfoxide (DMSO) first as a stock solution, and then added into the bath solution to a desired test concentration. DMSO concentration in the drug-containing solutions was limited to 0.3% (at this concentration DMSO does not have any effect on the ionic currents of interest).

Data Analysis Data were expressed as Mean \pm S.E. Paired Student's *t* test was used to evaluate the significance of the difference between the means before and after application of drugs. Analysis of Variance (*ANOVA*) was applied to evaluate the multiple group data. A value of $p < 0.05$ was accepted as a statistically significant level. Curve fittings and graphing were performed using Clampfit in pClamp 8.2 bundle (Axon Instruments, CA) and Origin v7.0 software (OriginLab Cooperation, Northampton, MA).

Results

Potentiation of the *hERG* current by PD-118057 and its analogs

PD-118057 was first examined for its effect on the *hERG* potassium channel in *hERG*-HEK cells. Currents were elicited by a voltage protocol described previously (Cordes et al., 2005; Volberg et al., 2002), which held the cell at -80 mV and stimulated at 0.25 Hz with a step pulse to $+20$ mV for 1 second followed by a 0.5 V/s ramp to -80 mV (Figure 1A inset). A slow but significant increase of the current amplitude was observed at 1, 3, and 10 μ M, respectively (Figure 1A-C, $n = 4\text{--}8$, $p < 0.01$). The holding current and series resistance were monitored to rule out the possibility of a recording artifact. The current traces obtained in the presence of the drug, both at depolarization and repolarization phases, almost paralleled that of the control, indicating no apparent kinetic change and involvement of the endogenous currents in HEK-293 cells. Indeed, PD-118057 was also tested in 3 wild-type HEK-293 cells, and showed either a negligible effect or a slight inhibition of the endogenous current (Figure 1D). Moreover, the increased current, when measured at the repolarization tail, can be completely blocked by a high concentration of dofetilide (10- μ M, Figure 1B), which was previously shown to have little effect on the endogenous current. The *hERG* current increase by PD-118057 at concentrations tested required at least 5 minutes to reach a steady state, and often led to loss of recordings after the current had been substantially elevated (average 111% increase in the tail current at 10 μ M, $n = 8$), therefore higher concentrations were not investigated. It is possible that the small HEK-293 cells were especially sensitive to the activation of the *hERG* potassium channel, since no apparent cytotoxicity was observed

MOLPHARM/2005/014035

following exposure to the compound at higher concentrations which were achieved in other *in vitro* and *in vivo* studies (data not shown).

Similar *hERG*-enhancing effects were observed in several structurally related analogs of PD-118057 (Table 1). Comparable or slightly stronger effects were noted with PD-198986, PD-307243 and PD-322388, while less potent effect was obtained with PD-202091. Virtually no effect was induced by PD-117780 and PD-201583 at 10 μM . The current traces after administration of these compounds demonstrated unchanged kinetics (data not shown) as did the experiments of PD-118057 (Figure 1A), indicating a similar mechanism of action. Due to cell survival and compound solubility issues at high concentrations, a full concentration-response relationship could not be established. No signs of “saturation” of the *hERG*-enhancing effect were indicated for PD-118057 at 10 μM although >100% increase of the *hERG* current was induced.

Additional mechanistic studies were completed using PD-118057 as a representative of the structural series. First, the voltage-dependent activation was investigated by using a series of 1-s depolarization pulses ranging from -70 to $+40$ mV from a holding potential (HP) of -80 mV (Figure 2A inset). Tail currents were elicited by a repolarization at -70 mV. The current amplitudes measured at the end of depolarization and the peak tail currents were averaged ($n = 6$) and plotted against membrane potentials, as shown in Figure 2B&C. Depolarization-activated currents increased with voltage initially and then decreased at voltages over -10 mV (Figure 2B), a characteristic of the *hERG* channel resulting from voltage-dependent C-type inactivation. PD-118057 at 3 μM increased the current at all voltages positive to -50 mV ($p < 0.05$). The voltage dependence of steady-state activation of the channel was described by fitting the tail

MOLPHARM/2005/014035

currents using a Boltzmann function (Figure 2C): $I/I_{\max} = 1 / \{1 + \exp[(V_{1/2} - V_m)/k]\}$, where I represents the tail current, V_m is the test membrane potential, $V_{1/2}$ is the half-maximal activation voltage, and k is the slope factor representing the steepness of the voltage dependence. No statistically significant difference was found in $V_{1/2}$ between PD-118057 (-31.4 ± 2.3 mV) and the control (-29.6 ± 2.2 mV), however a slightly steeper activation-voltage relationship was obtained in the presence of PD-118057 as indicated by an increased slope factor k (8.1 ± 1.1 mV vs. 6.1 ± 0.6 mV control, $n = 6$, $p < 0.05$).

The activation kinetics of the *hERG* channel in the presence and absence of 3 μ M PD-118057 was estimated by fitting the rising phase of the currents with a single exponential function. Acknowledging the methodological limitation of this approach at high membrane potentials because of an overlapping inactivation process (Zhou et al., 1998), we only applied curve fitting to the current traces obtained at $-40 \sim 10$ mV, when the fast inactivation posed minimal interference to the analysis of much slower activation kinetics. The resulting time constants demonstrated little difference between the drug and control groups (Figure 3B), indicating that PD-118057 did not affect activation kinetics of the *hERG* channel. Indeed, when the current sizes before and after drug administration were normalized, the two traces were superimposable (Figure 3A), including the deactivation (tail) current at -70 mV. Further investigation of the deactivation kinetics were performed in a separate experiment in which a series of 4-s repolarization steps was given following a 1-s depolarization pulse at $+60$ mV from HP of -80 mV. Deactivation kinetics at each voltage was then described using single or double exponentials, and the resulting fast and slow exponentials were averaged and plotted in Figure 3C. No major difference was found between the PD-118057 and

MOLPHARM/2005/014035

control groups ($n = 6$, $p > 0.05$). Using the same protocol, the recovery kinetics from inactivation was obtained by fitting the rising phase of the current upon repolarization with a single exponential function. The resulting time constants in relation to the membrane voltages were presented in Figure 3D, and the recovery phase of the current traces before and after application of PD-118057 were superimposable after the current amplitude was normalized (insets of Figure 3D). These results indicated that PD-118057 did not affect the recovery kinetics from steady-state inactivation. However, slightly slower inactivation kinetics was observed after treatment of 3 μ M PD-118057, represented by statistically significant increases in time constants at all testing voltages (Figure 4A). Here the currents were elicited by membrane potentials ranging from -40 to $+50$ mV, following a 200-ms pre-pulse at $+60$ mV and a 2-ms hyper-polarization at -100 mV. The current decay was then fitted with a single exponential. It should be noted that the instantaneous currents in these experiments were extremely large (often >10 nA post-drug). The details of the fast inactivation phase could easily be confounded by technical limitations (e.g. overlapping capacitance transient, voltage and dynamic voltage errors, etc.), making it difficult to accurately assess the kinetics. Therefore, we followed up the study at room temperature (22°C) when fewer channels were activated and the gating kinetics was slowed down. As shown in Figure 4B, no difference was seen in the time constants at any test potentials ($n = 5$, $p > 0.05$) under this recording condition. Another piece of supporting evidence was that, in a separate set of experiments, 3 μ M PD-198986, an equipotent close analogue of PD-118057 with 3-trifluoromethyl group replacing the 3-chlorine, did not exert any effect on the inactivation kinetics ($n = 4$, $p > 0.05$, Figure 4C) and other biophysical parameters (data not shown).

In Figure 5A and 5B, 3 μM PD-118057 was allowed to superfuse two cells separately while either being continuously stimulated (A) or held at -80 mV for 10 min before stimulation resumed (B). Similar extent of potentiation of the *hERG* current was observed after the pause of stimulation (B) as compared with the one with continuous stimulation (A), indicating that the *hERG*-enhancing effect of PD-118057 does not require open conformation of the channel.

PD-118057 does not affect I_{Na} , $I_{\text{Ca,L}}$, I_{K1} and I_{Ks} in guinea-pig ventricular myocytes

To examine if the effect of PD-118057 was selective to the *hERG* channel, we isolated ventricular myocytes from guinea-pig hearts and used whole-cell patch-clamp technique to record I_{Na} , $I_{\text{Ca,L}}$, I_{K1} and I_{Ks} currents. These are the major currents in shaping the action potential besides I_{Kr} . I_{Ca} was elicited by a 250-ms depolarization to $+10$ mV following a 200-ms pre-pulse at -40 mV to inactivate the T-type calcium current, if present. Cells were held at -70 mV. As shown in Figure 6A & 6B, ~ 5 -min application of 10 μM PD-118057 did not significantly affect the L-type calcium current. To record I_{Ks} , we held the myocytes at -40 mV and stimulated them with a series of 2-s depolarization pulses at -20 to $+60$ mV with a 20-mV increment (Figure 6C). The tail I_{Ks} current was elicited at -40 mV. The I_{K1} current illustrated in Figure 6D utilized a ramp voltage protocol (from -100 to $+50$ mV, 75 mV/s). To record I_{Na} , the extracellular Na^+ concentration was reduced to 15 mM and the holding potential was -120 mV. A series of depolarization pulses were applied, ranging from -100 to 0 mV. Similar to the results on the $I_{\text{Ca,L}}$, 10 μM PD-118057 did not produce any significant effect on I_{Ks} , I_{K1} and I_{Na} as shown in Figure 6C-E.

Effect of PD-118057 on action potential duration

The specific *hERG*-enhancing effect by PD-118057 indicates its ability to shorten the action potential duration in native cardiac myocytes. To test this hypothesis, we first recorded action potentials in guinea-pig ventricular myocytes by using the perforate-patch technique under current-clamping mode. Due to inherent technical limitations in achieving stable recordings of action potentials from single myocytes, we were unable to quantitate the effect. However, a trend of significant shortening was observed by PD-118057 at both 3 and 10 μM , as shown in Figure 6F for the current traces chosen from medians of the “steady-state” range of action potentials in an experiment. Similar results were observed in several other cells. To quantitatively determine the effect, we used floating electrodes to simultaneously record the action potentials from epicardial and endocardial sites and transmural ECG in arterially perfused rabbit ventricular wedge preparations at a frequency of 0.5 Hz. As shown in Figure 7A, perfusion with solutions containing 3 and 10 μM PD-118057 caused shortening of both epicardial and endocardial APDs and the QT interval on the transmural ECG. The effect normally developed slowly at 3 μM , could continue on for 2~3 hours and was difficult to wash off. At 10 μM , the shortening often progressed until no action potentials could be induced if no other intervention was allowed. Data shown in Figure 7A were chosen at ~2 hours after administration of 3 μM PD-118057 and ~30 min after 10 μM . Shortenings of epicardial APD₉₀, endocardial APD₉₀ and QT interval by 10.8 ± 1.1 , 17.7 ± 1.6 and $10.4 \pm 2.6\%$, respectively, were observed at 3 μM ; and by 26.0 ± 5.9 , 35.6 ± 6.0 and $25.6 \pm 1.6\%$, respectively, at 10 μM ($n = 4$). Apparently, the effect of PD-118057 was more dramatic

MOLPHARM/2005/014035

in the endocardial region than in the epicardial region, resulting in a decreased transmural dispersion of repolarization (Δ APD was 14 ± 7 and 7 ± 11 ms, respectively, at 3 and 10 μ M, *vs.* 39 ± 4 in control; Endo – Epi). At 10 μ M, PD-118057 could invert the normal heterogeneity to a shorter epicardial APD than endocardial APD, which was manifested as a missing or inverted T wave on the transmural ECG (Figure 7A).

PD-118057 Reverses Dofetilide-induced APD/QT prolongation and EADs

The shortening of APD and QT by PD-118057 indicated a potential of this compound in treating drug-induced QT prolongation and arrhythmias. As shown in Figure 7B&C, PD-118057 (right panel of 7B and closed circles in 7C) prevented the significant prolongation of APDs and QT interval caused by 3, 10 and 30 nM dofetilide, which was evident in the time-matched vehicle control (left panel of 7B and open circles in 7C). Similar results were observed in 3 more experiments (stimulation frequency: 1 Hz). In this study, 3 μ M PD-118057 or vehicle was present from 30 min before 3 nM dofetilide to the end of 30 nM dofetilide treatment. In the vehicle-treated preparation, dofetilide at 3, 10 and 30 nM produced epicardial APD₉₀ prolongations of 13, 32, and 56%, respectively, and endocardial APD₉₀ prolongations of 15, 35, and 59%, respectively. In contrast, in the preparation pretreated with 3 μ M PD-118057, dofetilide at 3, 10 and 30 nM only produced average changes of 5.6, 2, and –20% in the epicardial APD₉₀, respectively, and –1.5, –5.1 and –18.4% in endocardial APD₉₀, respectively. As compared with the effect of PD-118057 alone shown in Figure 7A, it appeared that PD-118057 was more effective in shortening the action potentials that had been prolonged. The lack of increase or even a decrease in APD by higher concentrations of dofetilide

MOLPHARM/2005/014035

most likely reflected a continuously increased effect of PD-118057 during the course of the experiment. It is worthy to note that dofetilide and other selective I_{Kr} blockers, such as *dl*-sotalol (Shimizu et al., 1999), increase the transmural dispersion of repolarization (TDR) by more prominently increasing the APD in endocardium (or M cells in large animals) than in epicardium (Figure 7B, vehicle group). PD-118057 3 μ M was shown to be effective in reversing this action, leading to a decreased TDR. Apparently over-corrected TDR could result in a shorter endocardial than epicardial APDs and missing or inverted T waves (Figure 7B).

In another set of experiments, the wedge was exposed to 10 nM dofetilide first while being stimulated at 0.5 Hz, a condition that typically facilitates the genesis of early afterdepolarization (EAD) (Joshi et al., 2004; Xu et al., 2003). As shown in Figure 8, a phase 2 EAD was clearly present in both epicardial and endocardial action potential waveforms after application of 10 nM dofetilide. The APD prolongation and EADs induced by dofetilide were shown in previous studies to persist during the course of an experiment if no intervention was given. Then we applied 3 μ M PD-118057 to the perfusate in the presence of dofetilide. After 1~2 hours of perfusion, the action potentials were almost restored to its control level and the EAD was completely eliminated. Similar results were obtained in two other experiments.

Discussion

PD-118057 and several of its analogs were shown in our study to significantly enhance the *hERG* current in HEK-293 cells within the test concentrations of 1-10 μM . No major changes were found in the gating and kinetic properties of the *hERG* channel by 3 μM PD-118057 except for a small but statistically significant slowing of the inactivation time course. This small change in the inactivation kinetics is most likely due to technical limitation in accurately measuring the super-fast inactivation process at 35°C, supported by the negative results from the room temperature experiment and from its close analog PD-198986 in a separate set of experiments.

The seven analogs reported in this paper possess differing potencies with respect to increasing the *hERG* channel current. While it is difficult to draw a conclusive structure-activity relationship (SAR) based on the limited number of compounds, it appears that both the electrostatic properties of molecules and the distance between the two phenyl rings may play a role in the effect. For example, both PD-307243 and PD-322388 have a 3,4-disubstitution pattern on the halogenated phenyl ring, similar to the substitution pattern of PD-118057 and PD-198986. Removal of the halogen groups from the phenyl ring resulted in a near complete loss of the *hERG*-enhancing activity, as what happened with PD-117780 and PD-201583. The major difference here is that the substituents on the “western” ring in these two compounds are electron-donating in character, compared to the other active analogs that have halogen substituents known to be electronegative. On the other hand, less effect was also induced by PD-202091 although it did have a halogenated phenyl ring. Apparently the lengthened linker (3 atoms) between the halogenated and the attached phenyl rings, compared to a 2-atom

MOLPHARM/2005/014035

linker in PD-118057 and PD-198986, resulted in a less optimal structure in exerting the *hERG*-enhancing effect.

The *hERG* potassium channel has been reported to be regulated by a number of intracellular molecules and pathways, including cAMP and protein kinase A (Cui et al., 2000; Thomas et al., 1999), protein kinase C (Barros et al., 1998; Thomas et al., 2004), phospholipase C (PLC) (Bian et al., 2001; Bian et al., 2004; Gomez-Varela et al., 2003), and *Src* tyrosine kinase (Cayabyab and Schlichter, 2002). Increase of the *hERG* current can be induced by the substrate of PLC, phosphatidyl inositol 4,5-bisphosphate (Bian et al., 2001; Bian et al., 2004), activation of *Src* tyrosin kinase (Cayabyab and Schlichter, 2002), and perhaps by modulations of other pathways. However, these regulatory mechanisms often lack specificity and, therefore, affect functions of other ion channels. In addition, regulations through these cellular processes are often associated with gating and/or kinetic changes, and the magnitude of the effect is often limited in cell lines (e.g. HEK-293) with only endogenous expression of these proteins, if present. While we cannot rule out the possibility that PD-118057 and its analogs act through indirect mechanisms to increase the *hERG* current, the unchanged biophysical property of the channel and such a dramatic enhancement of the current amplitude seem to support that PD-118057 is able to bind to the channel directly and increase its open probability. Further work at the single-channel level should help to confirm this hypothesis.

The magnitude of the *hERG* current potentiation by these compounds and the mechanism, if proved, appeared to contrast drastically with RPR260243, another *hERG* enhancer reported very recently (Kang et al., 2005). At 10 μ M, PD-118057 produced an average of 111% increase of the *hERG* current, compared to only 15% by RPR260243 at

MOLPHARM/2005/014035

the same concentration. RPR260243 dramatically slowed the deactivation kinetics but PD-118054 had basically no major effect on gating or kinetic properties of the *hERG* channel. PD-118057 significantly shortened the action potential duration at tested concentrations (3-10 μM) in guinea-pig ventricular myocytes but RPR260243 had almost no effect until 30 μM . Similar to RPR260243 in the guinea-pig myocytes but more effectively, PD-118057 at 3 μM was able to prevent and treat 10 nM dofetilide-induced APD or QT prolongation, increased heterogeneity of repolarization and phase 2 EAD in arterially perfused rabbit left ventricular wedge. Phase 2 EADs are believed to be the major mechanism of the triggered activity responsible for initiation of the arrhythmia, and the increased TDR is considered to be a substrate for reentry responsible for maintenance of the arrhythmia (Antzelevitch, 2004; Shryock et al., 2004). Both parameters can be easily monitored in the ventricular wedge preparation (Antzelevitch, 2004; Joshi et al., 2004; Medina-Ravell et al., 2003; Shimizu et al., 1999), and shown to be highly predictive to the clinical outcome of drug-induced arrhythmia. Therefore, our study results have undoubtedly provided important preclinical evidence that potentiation of the *hERG* potassium channel by a pharmaceutical might be beneficial to individuals with delayed repolarization. Potential therapeutic indications may include prevention and treatment of arrhythmias in patients with LQTS (congenital or acquired), congestive heart failure and diabetes. Combinations of these compounds with QT-prolonging agents may potentially mitigate their adverse cardiac effects while retaining their benefits. On the other hand, it should also be noted that PD-118057 could cause QT interval shortening and decrease the normal heterogeneity of repolarization in rabbit ventricular wedge. It is unclear at this stage whether this effect observed *in vitro* would translate to a

MOLPHARM/2005/014035

proarrhythmic risk in man. Obviously more investigative work is necessary to further assess the potential therapeutic value and safety profile of PD-118057 and its analogs.

Acknowledgement

The authors wish to thank Dr. Mei-Hua Tu for helpful discussions in part of the work. We also wish to acknowledge Annette Sakkab-Tan, Chung Choi, and Yingjie Lai for the synthesis of test compounds. These compounds were made through a collaboration with Yamanouchi Pharmaceutical Company, Ltd.

Reference

- Antzelevitch C (2004) Cellular basis and mechanism underlying normal and abnormal myocardial repolarization and arrhythmogenesis. *Ann Med* **36 Suppl 1**:5-14.
- Barros F, Gomez-Varela D, Vilorio CG, Palomero T, Giraldez T and de la Pena P (1998) Modulation of human erg K⁺ channel gating by activation of a G protein-coupled receptor and protein kinase C. *J Physiol* **511 (Pt 2)**:333-46.
- Bian J, Cui J and McDonald TV (2001) HERG K(+) channel activity is regulated by changes in phosphatidyl inositol 4,5-bisphosphate. *Circ Res* **89**:1168-76.
- Bian JS, Kagan A and McDonald TV (2004) Molecular analysis of PIP₂ regulation of HERG and IKr. *Am J Physiol Heart Circ Physiol* **287**:H2154-63.
- Cayabyab FS and Schlichter LC (2002) Regulation of an ERG K⁺ current by Src tyrosine kinase. *J Biol Chem* **277**:13673-81.
- Cordes JS, Sun Z, Lloyd DB, Bradley JA, Opsahl AC, Tengowski MW, Chen X and Zhou J (2005) Pentamidine reduces hERG expression to prolong the QT interval. *Br J Pharmacol* **145**:15-23.
- Cui J, Melman Y, Palma E, Fishman GI and McDonald TV (2000) Cyclic AMP regulates the HERG K(+) channel by dual pathways. *Curr Biol* **10**:671-4.
- De Ponti F, Poluzzi E and Montanaro N (2000) QT-interval prolongation by non-cardiac drugs: lessons to be learned from recent experience. *Eur J Clin Pharmacol* **56**:1-18.
- De Ponti F, Poluzzi E and Montanaro N (2001) Organising evidence on QT prolongation and occurrence of Torsades de Pointes with non-antiarrhythmic drugs: a call for consensus. *Eur J Clin Pharmacol* **57**:185-209.
- Fermini B and Fossa AA (2003) The impact of drug-induced QT interval prolongation on drug discovery and development. *Nat Rev Drug Discov* **2**:439-47.
- Gomez-Varela D, Barros F, Vilorio CG, Giraldez T, Manso DG, Dupuy SG, Miranda P and de la Pena P (2003) Relevance of the proximal domain in the amino-terminus of HERG channels for regulation by a phospholipase C-coupled hormone receptor. *FEBS Lett* **535**:125-30.
- Joshi A, Dimino T, Vohra Y, Cui C and Yan GX (2004) Preclinical strategies to assess QT liability and torsadogenic potential of new drugs: the role of experimental models. *J Electrocardiol* **37 Suppl**:7-14.
- Kang J, Chen XL, Wang H, Ji J, Cheng H, Incardona J, Reynolds W, Viviani F, Tabart M and Rampe D (2005) Discovery of a Small Molecule Activator of the Human Ether-a-go-go-Related Gene (HERG) Cardiac K⁺ Channel. *Mol Pharmacol* **67**:827-36.
- Medina-Ravell VA, Lankipalli RS, Yan GX, Antzelevitch C, Medina-Malpica NA, Medina-Malpica OA, Droogan C and Kowey PR (2003) Effect of epicardial or biventricular pacing to prolong QT interval and increase transmural dispersion of repolarization: does resynchronization therapy pose a risk for patients predisposed to long QT or torsade de pointes? *Circulation* **107**:740-6.
- Shimizu W, McMahon B and Antzelevitch C (1999) Sodium pentobarbital reduces transmural dispersion of repolarization and prevents torsades de Pointes in models of acquired and congenital long QT syndrome. *J Cardiovasc Electrophysiol* **10**:154-64.

- Shryock JC, Song Y, Wu L, Fraser H and Belardinelli L (2004) A mechanistic approach to assess the proarrhythmic risk of QT-prolonging drugs in preclinical pharmacologic studies. *J Electrocardiol* **37 Suppl**:34-9.
- Sun Z, Milos PM, Thompson JF, Lloyd DB, Mank-Seymour A, Richmond J, Cordes JS and Zhou J (2004) Role of a KCNH2 polymorphism (R1047 L) in dofetilide-induced Torsades de Pointes. *J Mol Cell Cardiol* **37**:1031-9.
- Thomas D, Wu K, Wimmer AB, Zitron E, Hammerling BC, Kathofer S, Lueck S, Bloehs R, Kreye VA, Kiehn J, Katus HA, Schoels W and Karle CA (2004) Activation of cardiac human ether-a-go-go related gene potassium currents is regulated by alpha(1A)-adrenoceptors. *J Mol Med* **82**:826-37.
- Thomas D, Zhang W, Karle CA, Kathofer S, Schols W, Kubler W and Kiehn J (1999) Deletion of protein kinase A phosphorylation sites in the HERG potassium channel inhibits activation shift by protein kinase A. *J Biol Chem* **274**:27457-62.
- Volberg WA, Koci BJ, Su W, Lin J and Zhou J (2002) Blockade of human cardiac potassium channel human ether-a-go-go-related gene (HERG) by macrolide antibiotics. *J Pharmacol Exp Ther* **302**:320-7.
- Xu X, Yan GX, Wu Y, Liu T and Kowey PR (2003) Electrophysiologic effects of SB-237376: a new antiarrhythmic compound with dual potassium and calcium channel blocking action. *J Cardiovasc Pharmacol* **41**:414-21.
- Zabel M, Hohnloser SH, Behrens S, Li YG, Woosley RL and Franz MR (1997) Electrophysiologic features of torsades de pointes: insights from a new isolated rabbit heart model. *J Cardiovasc Electrophysiol* **8**:1148-58.
- Zhou Z, Gong Q, Ye B, Fan Z, Makielski JC, Robertson GA and January CT (1998) Properties of HERG channels stably expressed in HEK 293 cells studied at physiological temperature. *Biophys J* **74**:230-41.

Figure Legend:

Figure 1. PD-118057 potentiates the *hERG* current in stably expressed HEK-283

cells. A) Representative current traces before and after 1, 3, and 10 μM PD-118057. The *hERG* current was elicited by a 1-s depolarization pulse followed by a 0.5 V/s ramp to the holding potential of -80 mV. B) Time course of the effect of PD-118057 on the *hERG* current from a representative cell as shown in panel A. Current amplitude was measured at the peak tail current during the ramp repolarization phase. Dofetilide (10 μM) was applied at the end of experiment to evaluate possible endogenous and leakage currents. C) Summary of the concentration-dependent potentiation of the *hERG* current amplitude by PD-118057. Data were averaged from 4, 5, and 8 cells, respectively, for 1, 3, and 10 μM drug. $*p < 0.05$; $**p < 0.001$. D) Effect of 10 μM PD-118057 on the endogenous depolarization-activated outward current in wild-type HEK-293 cells. Currents were elicited by the same voltage protocol as used for the *hERG* current. Similar results were obtained from two more experiments.

Figure 2. Effects of PD-118057 on the current-voltage (I-V) relationship of the

***hERG* current.** A) Current traces recorded before and after application of 3 μM PD-118057. Cells were held at -80 mV. Depolarization steps ranging from -70 and $+40$ mV with 10-mV increments for 1 s were delivered to activate the channel, then a repolarization at -70 mV was given to elicit the tail current. B) I-V relationship before and after 3 μM PD-118057. Currents were measured at the end of the depolarization pulses. C) Effect of 3 μM PD-118057 on the voltage dependence of steady-state activation. Peak tail currents were measured upon repolarization and normalized.

MOLPHARM/2005/014035

Averaged data from 6 experiments were fitted with a Boltzmann function, resulting in a half-activation voltage and a slope factor of -31.6 and 8.4 mV, respectively, for PD-118057 and -29.8 and 6.6 mV, respectively for control.

Figure 3. PD-118057 did not affect activation, deactivation or recovery kinetics. A)

When normalized to size, currents recorded in the presence of $3 \mu\text{M}$ PD-118057 (light gray dotted) were almost superimposable to those in the control (black). B) Activation time constants at various membrane potentials before and after application of $3 \mu\text{M}$ PD-118057. A single exponential was used to fit the activation time course. $n = 6$. C) Deactivation kinetics was described using double or single exponential functions. Open symbols denote fast (\circ) and slow (\square) time constants under control and the closed symbols represent fast (\bullet) and slow (\blacksquare) time constants in the presence of PD-118057. Currents were elicited by a series of 4-s repolarization pulses ranging from -100 to $+50$ mV, following a 1-s depolarization at $+60$ mV. $n = 6$. Part of the current traces in response to various voltages (-100 to $+20$ mV, in 20 mV increments for clarity purpose) were shown in the inset. D) Recovery kinetics from steady-state inactivation was described by fitting the current rising phase with a single exponential. Normalized current traces before (black) and after (gray) application of $3 \mu\text{M}$ PD-118057 were almost superimposable, as demonstrated in the inset for traces at -20 and -100 mV (at different time scales for clarity purpose). Time constants data were obtained from 3 experiments. Note a large variation was observed at -90 mV which was close to the reversal potential, when only a small current was elicited.

Figure 4. Effect of PD-118057 and PD-198986 on the inactivation kinetics. A)

Inactivation time constants obtained from experiments run at 35°C . The current was

MOLPHARM/2005/014035

elicited by a series of voltages ranging from -40 to $+50$ mV, following a 200-ms prepulse at $+60$ mV and a 2-ms hyperpolarization at -100 mV. Current decay was fitted with a single exponential and the resulting time constants from 6 experiments were plotted against membrane potentials. B) Inactivation time constants obtained from 5 experiments at room temperature (22°C). Currents were elicited by a 250-ms prepulse at $+60$ mV, followed by a 2-ms hyperpolarization at -100 mV and the testing pulses at various potentials. C) Effect of $3\ \mu\text{M}$ PD-198986 on inactivation kinetics of the *hERG* channel. Data were obtained in a separate group of experiments ($n = 4$), in which different recording systems had been employed. Experiments were conducted at 35°C .

Figure 5. The hERG-enhancing effect of PD-118057 does not require channels to open.

A) Time course of the peak tail current in the presence of $3\ \mu\text{M}$ PD-118057. The *hERG* current was elicited by a step pulse of 1 second at $+20$ mV from holding potential of -80 mV, followed by a repolarization ramp to -80 mV at 0.5 V/s. B) A 10-min pause of stimulation was allowed following the administration of PD-118057. Note the tail current amplitudes after resuming the stimulation were enhanced to a similar extent to that in panel A. Boxes show the duration of the drug application. Dotted lines show the linear fit to the steady-state control for anticipated current levels when no drug intervention was given.

Figure 6. Effects of PD-118057 on $I_{\text{Ca,L}}$, I_{K1} , I_{Ks} and I_{Na} and action potential recorded from single guinea-pig cardiomyocytes.

A&B) L-type calcium current was elicited by a depolarization at 10 mV from -40 mV prepulse. Cells were held at -70 mV. Current traces before and after application of PD-118057 was shown in panel A, and the time course of current amplitudes measured at the peak $I_{\text{Ca,L}}$ shown in panel B. C, D & E)

MOLPHARM/2005/014035

Effects of PD-118057 on I_{Ks} , I_{K1} and I_{Na} , respectively. Both I_{Ks} and I_{K1} were recorded at 35°C, with a holding potential of -40 mV. I_{Ks} was elicited by a series of depolarization pulses ranging from -20 to +60 mV with an increment of 20 mV (C). I_{K1} was represented by a ramp protocol-elicited I-V trace. I_{Na} was recorded by using a series of 20-ms depolarization pulses (-100~0 mV) from a holding potential of -120 mV. F) PD-118057 shortened the action potential duration. Ctrl, 3 and 10 denote before and after application of 3 μ M and 10 μ M PD-118057, respectively. Since action potential durations varied in a range even during a steady state, traces were chosen from the ones with median APD among each “steady-state” range of action potentials.

Figure 7. Effects of PD-118057 on APD and QT interval in arterially perfused rabbit ventricular wedge. A) Epicardial and endocardial action potentials and transmural ECGs from a representative experiment was shown in the left panel. Average shortenings of APD₅₀, APD₉₀ and QT interval from 4 experiments were shown in the right panel. Data were collected ~2 hours after perfusion with 3 μ M and ~30 min after 10 μ M PD-118057. Numbers on the X-axis denote concentrations of the compound. B) Effect of dofetilide on action potential and ECG parameters in a representative tissue co-treated with 3 μ M PD-118057 or vehicle. Stimulation frequency: 1.0 Hz. C) Time course of epicardial and endocardial APD₉₀ in vehicle (open circles) or PD-118057 (closed circles) co-treatment groups. Numbers 0 ~ 5 in panels B&C denote control (0), perfusion with PD-118057 or vehicle (1), addition of 3 μ M (2), 10 μ M (3) and 30 μ M (4) dofetilide in the presence of PD-118057 or vehicle, and washout (5). For clarity purpose, traces in vehicle or PD-118057 pretreatment (1) and washout (5) groups were not shown in 7B.

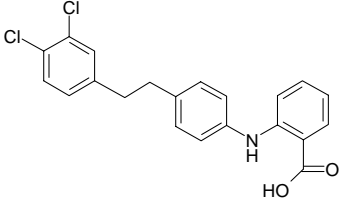
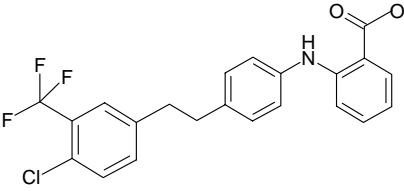
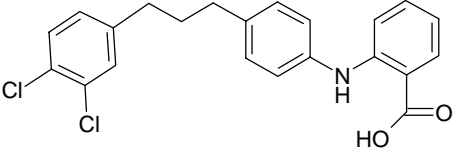
MOLPHARM/2005/014035

Figure 8. PD-118057 eliminated early after depolarization induced by 10 nM

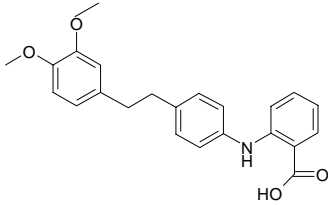
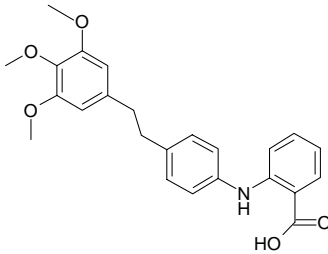
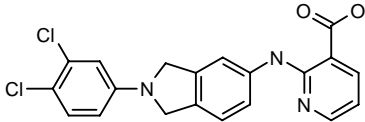
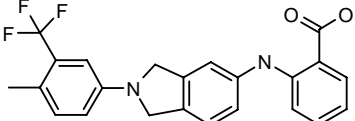
dofetilide. Epicardial and endocardial action potentials were recorded simultaneously at 0.5 Hz from an arterially perfused rabbit ventricular wedge. After establishing a baseline control (0), 10 nM dofetilide was applied to the wedge until a significant prolongation of APD was evident and an EAD was induced (1). Subsequently, 3 μ M PD-118057 was administered in the presence of dofetilide, and the waveform shown here (2) was collected after ~2 hours of perfusion.

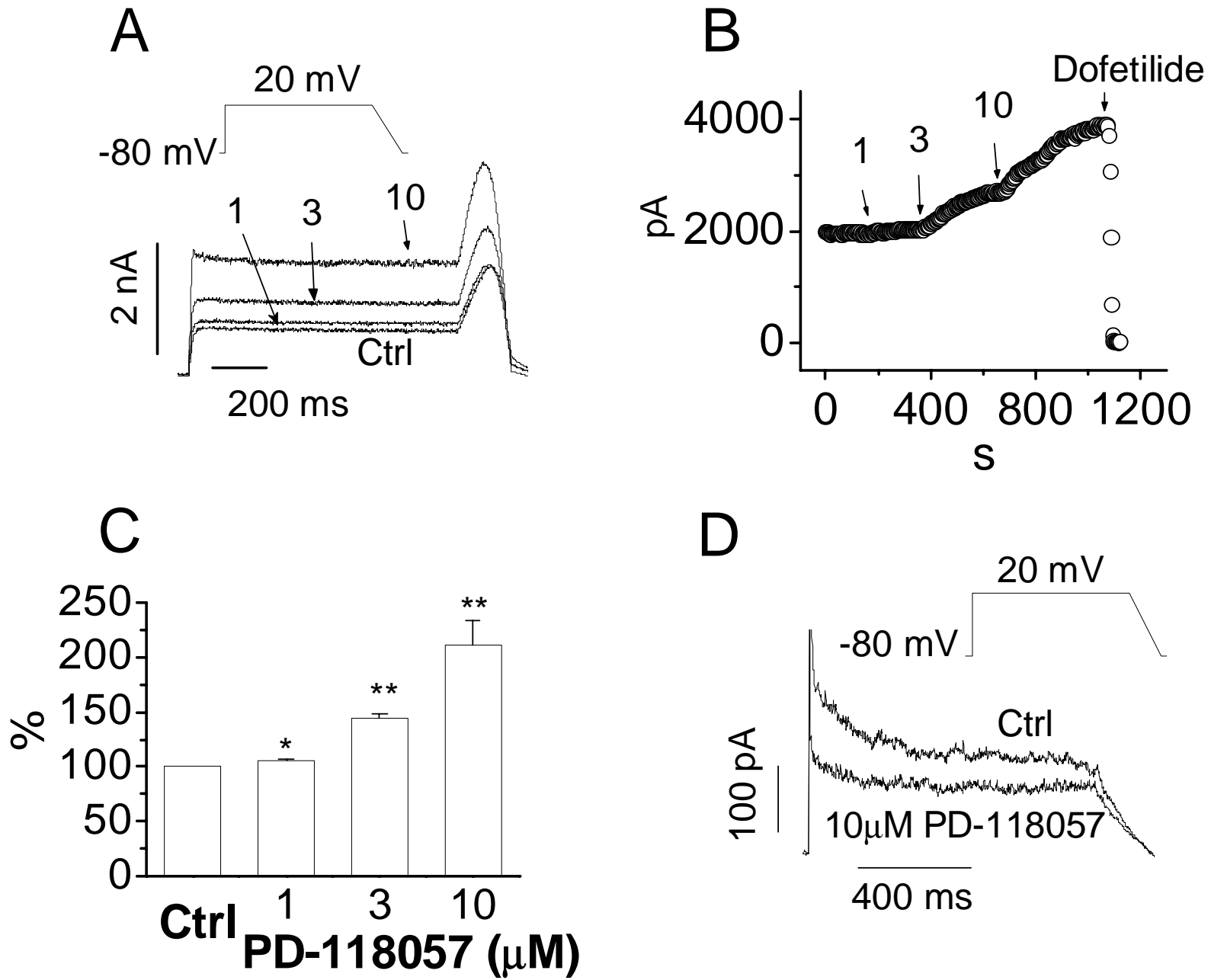
Table 1

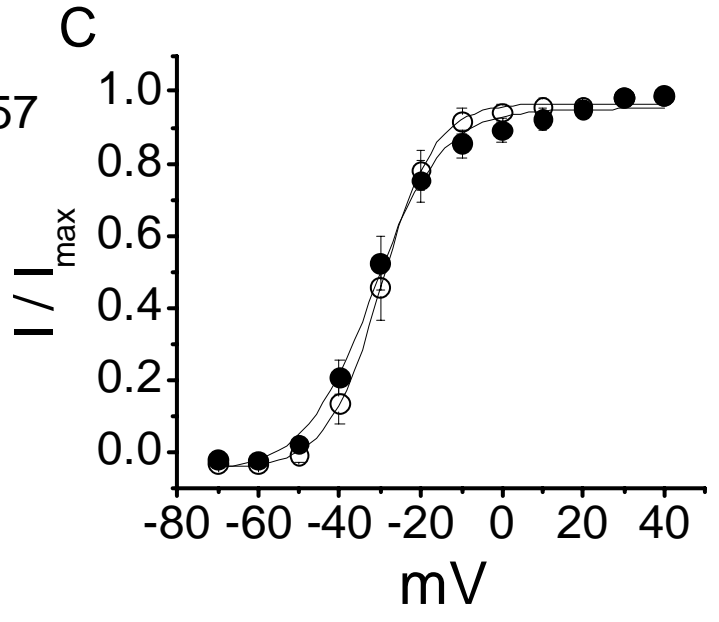
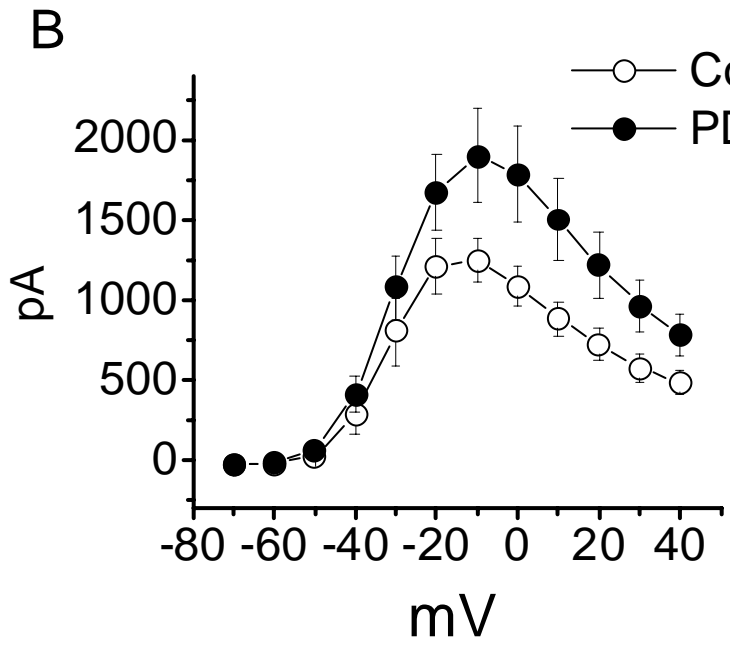
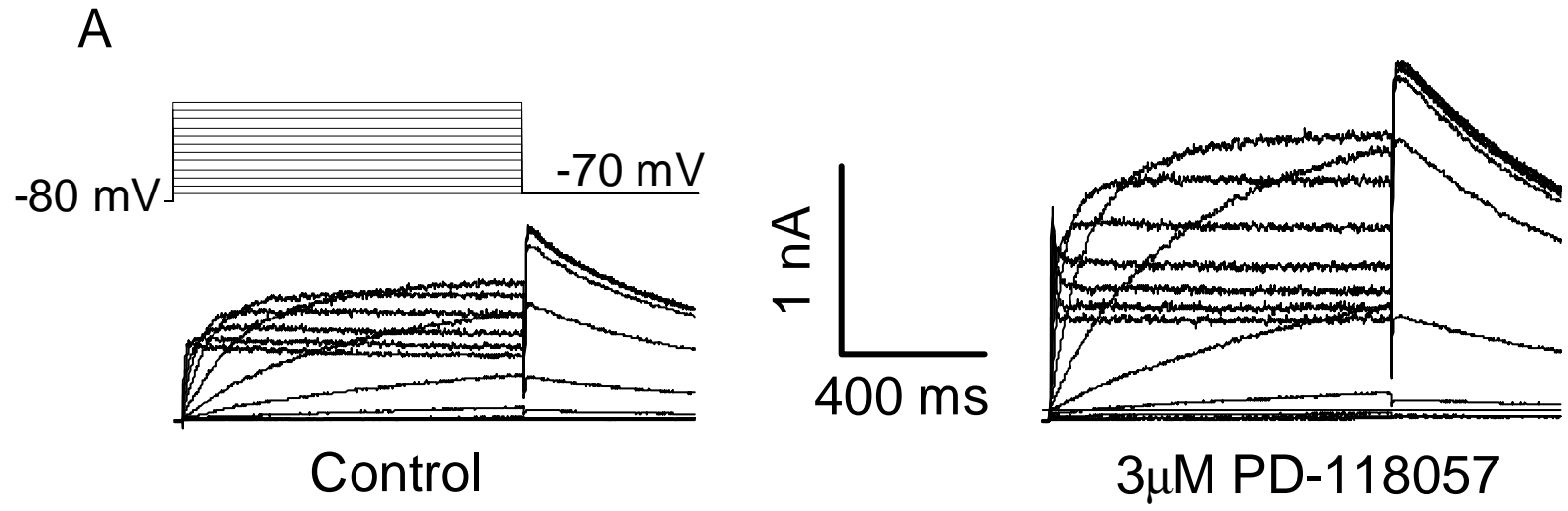
Compound structures and their *hERG*-enhancing activities. Percent increase of the peak tail current was calculated. Currents were elicited by using a voltage protocol shown in Figure 1. Mean \pm SE, $n = 4-8$.

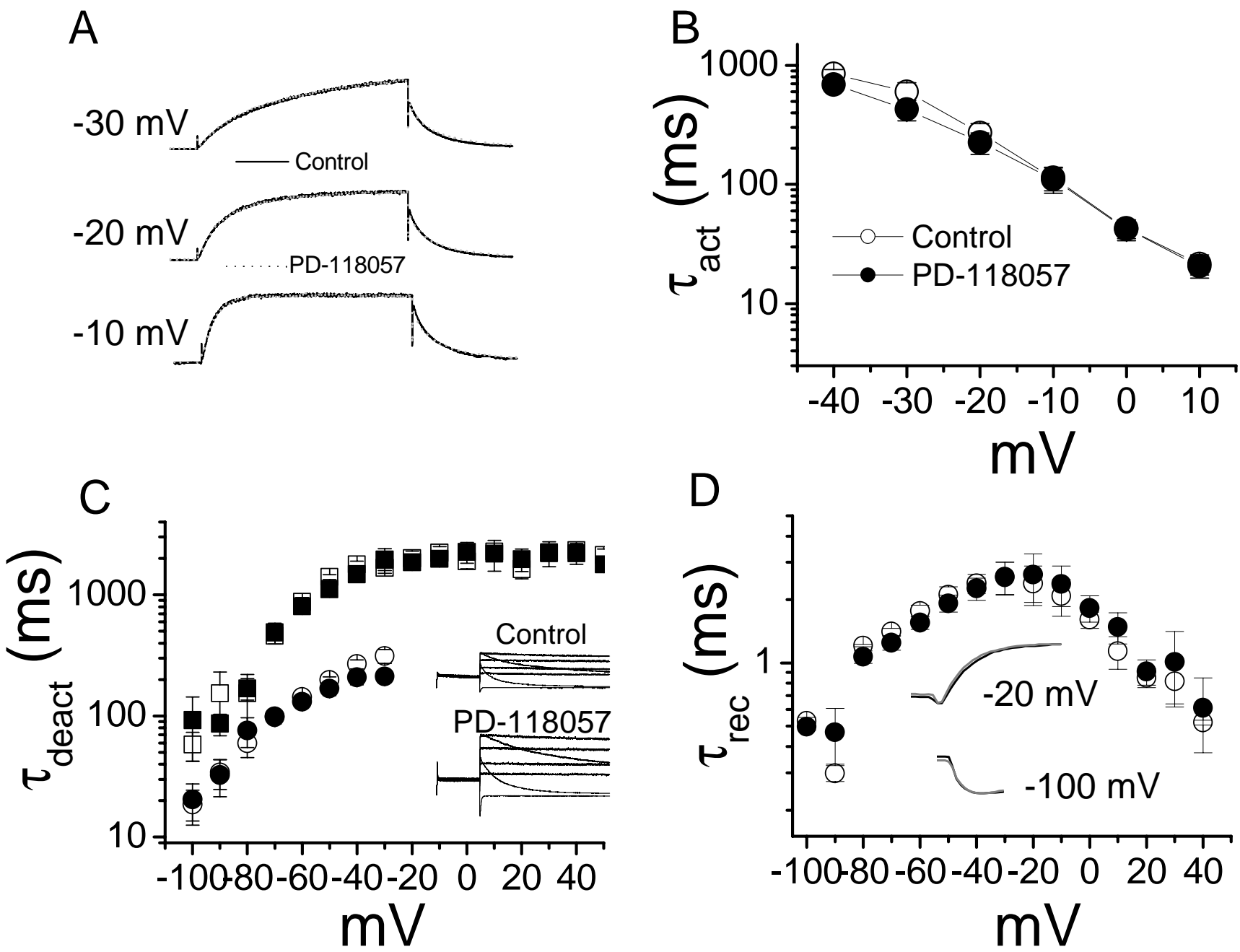
Compound	Structure	<i>hERG</i> Current Increase (at 10 μM)
PD-118057		111 \pm 22%
PD-198986		117 \pm 17%
PD-202091		19 \pm 3%

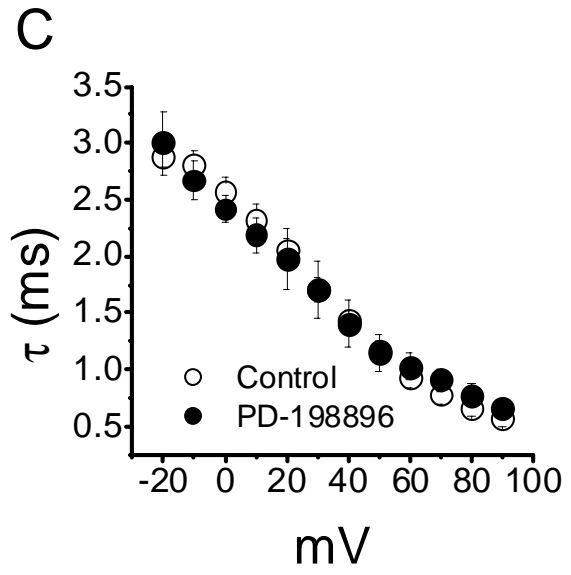
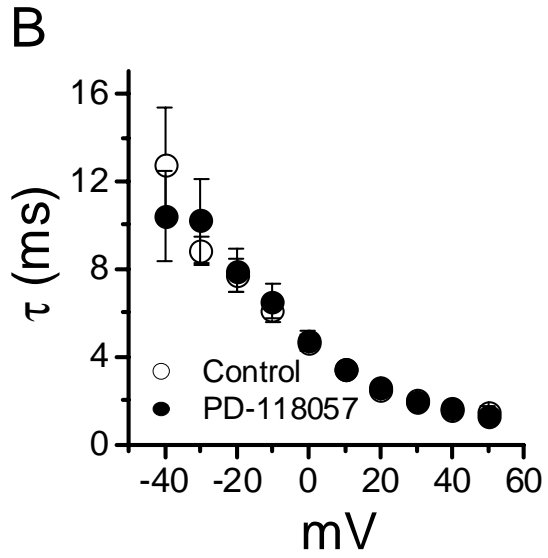
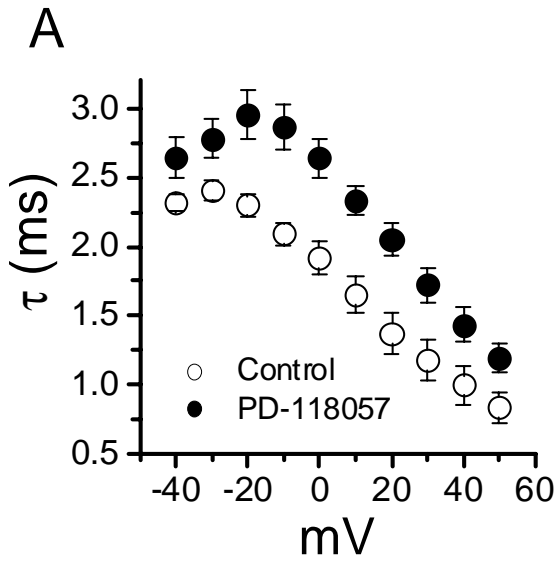
MOLPHARM/2005/014035

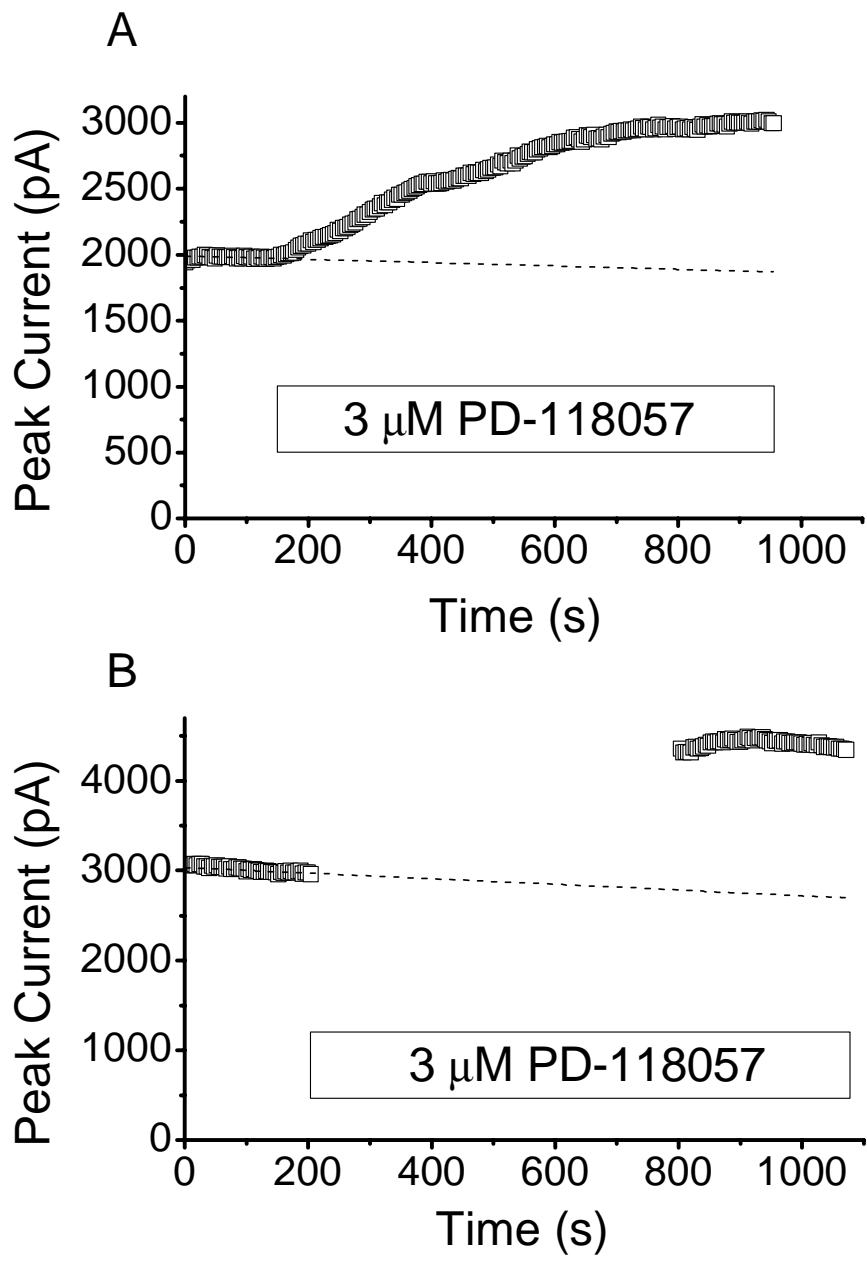
PD-117780		$0.4 \pm 2.6\%$
PD-201583		-4.0% ($n = 2$)
PD-307243		$58.3 \pm 9.1\%$ (at $1 \mu\text{M}$)
PD-322388		$191 \pm 23\%$

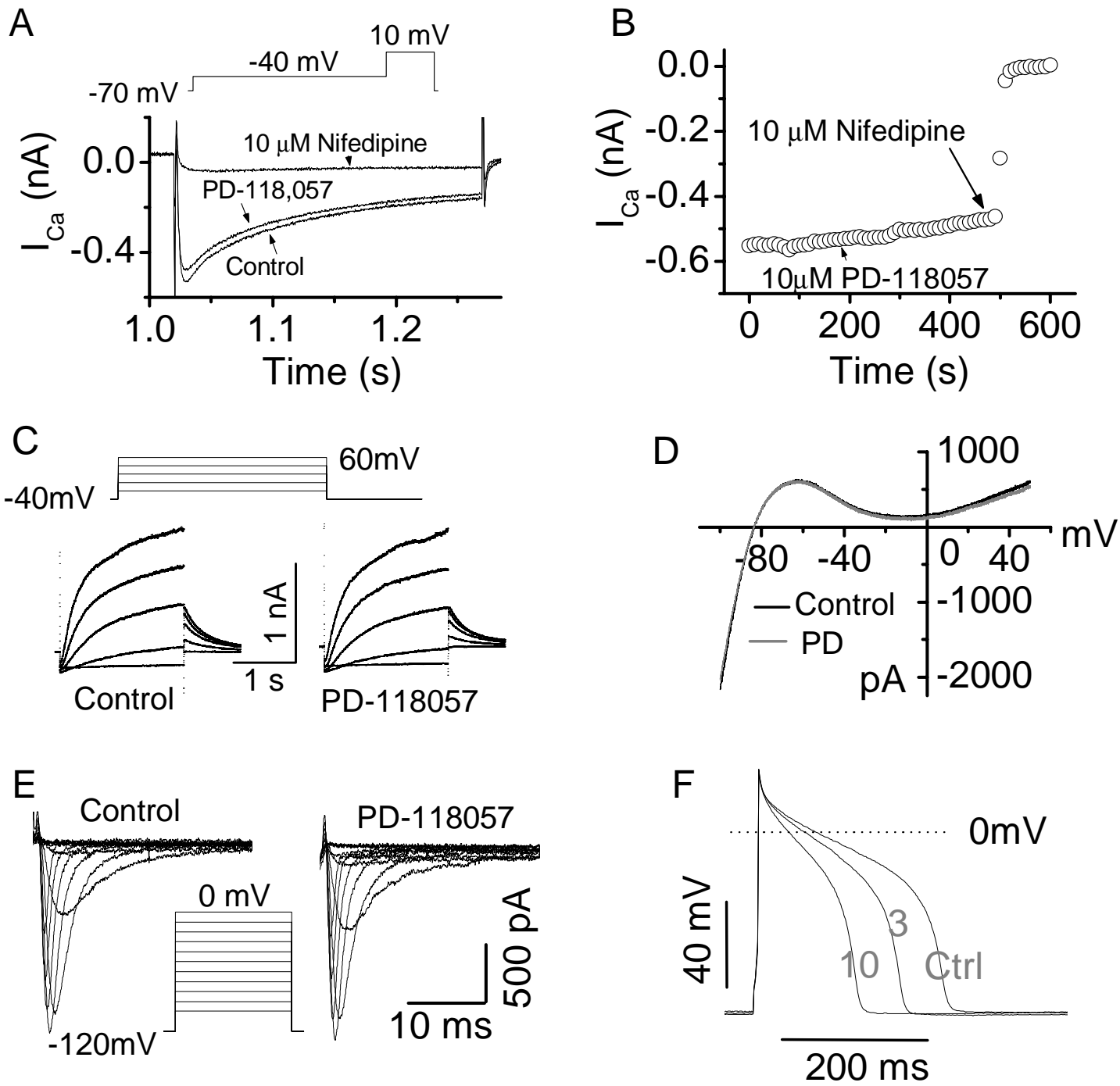




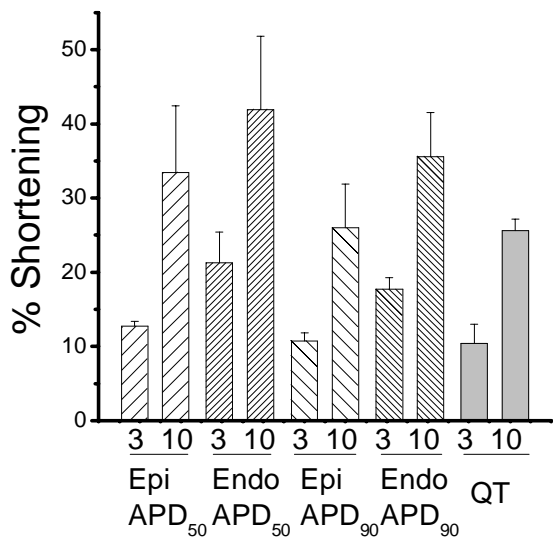
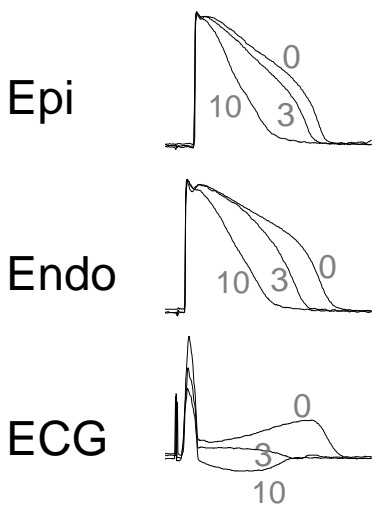




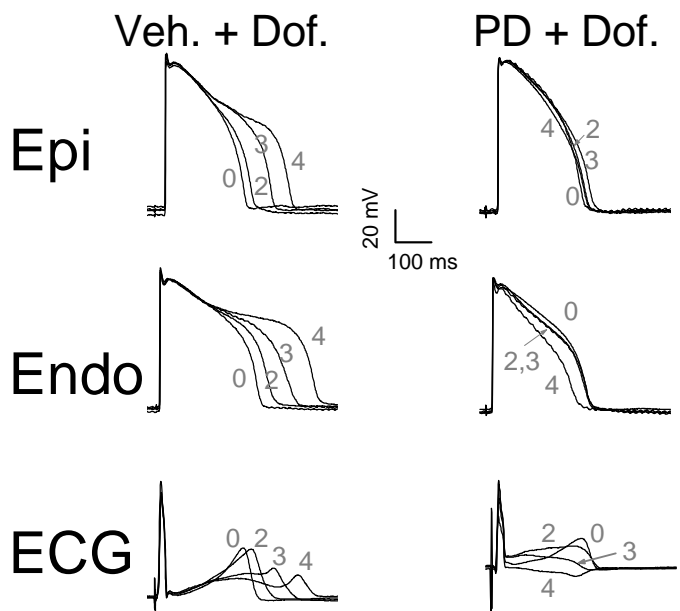




A



B



C

